Molecular Characterization of Insulin-Mediated Suppression of Hepatic Glucose Production In Vivo

Christopher J. Ramnanan,[1] Dale S. Edgerton,[1] Noelia Rivera,[1] Jose Irimia-Dominguez,[2] Ben Farmer,[1] Doss W. Neal,[1] Margaret Lautz,[1] E. Patrick Donahue,[1] Catalina M. Meyer,[2] Peter J. Roach,[2] and Alan D. Cherrington[1]

OBJECTIVE—Insulin-mediated suppression of hepatic glucose production (HGP) is associated with sensitive intracellular signaling and molecular inhibition of gluconeogenic (GNG) enzyme mRNA expression. We determined, for the first time, the time course and relevance (to metabolic flux) of these molecular events during physiological hyperinsulinemia in vivo in a large animal model.

RESEARCH DESIGN AND METHODS—24 h fasted dogs were infused with somatostatin, while insulin (basal or 8× basal) and glucagon (basal) were replaced intraportally. Euglycemia was maintained and glucose metabolism was assessed using tracer, ^2H_2O, and arterio-venous difference techniques. Studies were terminated at different time points to evaluate insulin signaling and enzyme regulation in the liver.

RESULTS—Hyperinsulinemia reduced HGP due to a rapid transition from net glycogen breakdown to synthesis, which was associated with an increase in glycogen synthase and a decrease in glycogen phosphorylase activity. Thirty minutes of hyperinsulinemia resulted in an increase in phospho-FOXO1, a decrease in GNG enzyme mRNA expression, an increase in $F2,6P_2$, a decrease in fat oxidation, and a transient decrease in net GNG flux. Net GNG flux was restored to basal by 4 h, despite a substantial reduction in PEPCK protein, as gluconeogenically-derived carbon was redirected from lactate efflux to glycogen deposition.

CONCLUSIONS—In response to acute physiologic hyperinsulinemia, *1*) HGP is suppressed primarily through modulation of glycogen metabolism; *2*) a transient reduction in net GNG flux occurs and is explained by increased glycolysis resulting from increased $F2,6P_2$ and decreased fat oxidation; and *3*) net GNG flux is not ultimately inhibited by the rise in insulin, despite eventual reduction in PEPCK protein, supporting the concept that PEPCK has poor control strength over the gluconeogenic pathway in vivo. ***Diabetes*** **59:1302–1311, 2010**

From the [1]Department of Molecular Physiology, Vanderbilt University School of Medicine, Nashville, Tennessee; and the [2]Department of Biochemistry and Molecular Biology, Indiana University School of Medicine, Indianapolis, Indiana.

Corresponding author: Christopher J. Ramnanan, chris.ramnanan@vanderbilt.edu.

Received 3 November 2009 and accepted 9 February 2010. Published ahead of print at http://diabetes.diabetesjournals.org on 25 February 2010. DOI: 10.2337/db09-1625.

Insulin acutely inhibits hepatic glucose production (HGP) in vivo by inhibiting glucose formation from both glycogenolysis and gluconeogenesis (GNG). Metabolic data in dogs and humans indicate that glycogenolytic flux is sensitively inhibited by physiological hyperinsulinemia, but gluconeogenic flux is not (1–8). These data suggest that insulin inhibits the gluconeogenic component of glucose production by diverting gluconeogenically derived glucose-6-phosphate (G6P) to glycogen, rather than suppressing gluconeogenic formation of G6P (GNG flux-to-G6P). Conversely, data from in vitro studies and in vivo studies in rodents have shown that insulin-mediated mechanisms inhibit both the glycogenolytic and gluconeogenic pathways at the enzymatic level. Insulin inhibits glycogen phosphorylase and stimulates glycogen synthase, facilitating the transition of the liver from glycogen breakdown to synthesis (9). Insulin also inhibits the gene expression of PEPCK and G6Pase, enzymes often described as rate-limiting in the GNG pathway. The CREB-regulated transcription coactivator-2 (CRTC2) drives the expression of PGC1α, and PGC1α interacts with FOXO1 to promote GNG gene expression (10–12). Hepatic insulin action results in the phosphorylation of CRTC2 and FOXO1, which excludes these proteins from the nucleus and reduces PEPCK and G6Pase gene expression (10–12). Recently, it has been suggested that insulin action in the brain also plays a role in suppressing GNG (13–15). It has been proposed that a rise in hypothalamic insulin modifies vagal input to the liver, leading to the phosphorylation of STAT3, which then inhibits GNG gene expression (13).

Since the biochemistry of GNG regulation has largely been established in rodent systems, the question arises as to whether it is applicable to large animals and humans. The molecular regulation of GNG by insulin in vivo has not been well characterized in humans due to the invasiveness of sampling human liver and the inaccessibility of the portal vein. The canine model offers the experimental opportunity to deliver insulin via the portal vein, to measure net balance of gluconeogenic substrates and glucose across the liver, and to obtain liver tissue for molecular characterization in a model that has proven to have high translational value to humans (16). Our aim was to characterize, for the first time, the time course of relevant insulin-mediated molecular events during the suppression of HGP by selective physiological (approximately eightfold) hyperinsulinemia in the conscious dog and to correlate these molecular changes with alterations in metabolic flux. The pancreatic clamp technique was used to isolate the effects of a selective rise in insulin in the presence of euglycemia and basal glucagon. Dogs were fasted for 24 h to create a situation in which the basal rates

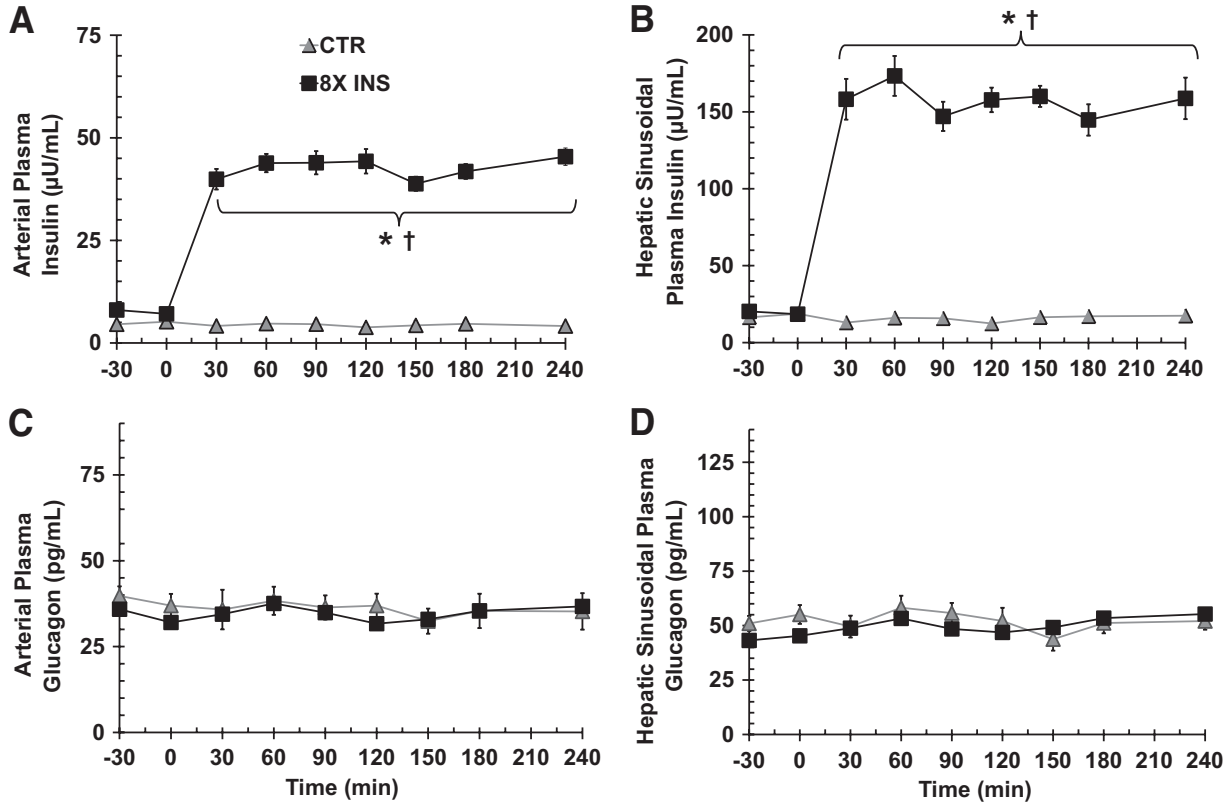

FIG. 1. Arterial plasma insulin (*A*), hepatic sinusoidal plasma insulin (*B*), arterial plasma glucagon (*C*), and hepatic sinusoidal plasma glucagon concentrations (*D*) in 24 h fasted conscious dogs during the basal (−30 to 0 min) and experimental (0–240 min) periods. Data are means ± SEM; $n = 7$ in control (CTR) and $n = 20$ in 8× insulin (8X INS) groups. *$P < 0.05$ vs. CTR group; †$P < 0.05$ vs. basal period.

of gluconeogenic and glycogenolytic flux better reflect those in the overnight fasted human. Studies were ended after different durations of hyperinsulinemia, at which time liver samples were obtained for the measurement of molecular markers. Control animals were not exposed to elevated insulin but were otherwise treated the same.

RESEARCH DESIGN AND METHODS

Animal care and surgical procedures. Adult dogs of either sex, with a mean weight of 21.9 ± 0.2 kg at time of study, were housed and fed as described previously (5) and then studied after a 24 h fast. The surgical facility met the standards published by the American Association for the Accreditation of Laboratory Animal Care, and the protocols met the approval of the Vanderbilt University Medical Center Animal Care Committee. Two weeks before experimentation, all dogs underwent a laparotomy to implant sampling catheters into the femoral artery, the portal vein, and the hepatic vein, to place infusion catheters in the splenic and jujenal veins, and to place ultrasonic flow probes (Transonic Systems, Ithaca, NY) around the hepatic artery and the portal vein, as described previously (5). All dogs were healthy, as indicated by *1*) leukocyte count <18,000/mm^3, *2*) hematocrit >35%, and *3*) good appetite and normal stools.

Experimental design. Each study consisted of an equilibration (−150 to −30 min), a basal (−30 to 0 min), and an experimental period (0.5, 1, 2, or 4 h). At −150 min, salinized ^2H_2O (3 ml/kg; Sigma) was administered intravenously in a subset of animals in each group ($n = 3$ control and $n = 5$ experimental) to achieve ~0.55% enrichment of body water. All animals were carefully monitored during the experiments, and no adverse effects of ^2H_2O administration were detected. At −120 min, a priming dose of [3-^{3}H]glucose (35 μCi) was given, followed by a constant infusion of [3-^{3}H]glucose (0.35 μCi/min). At the beginning of the experimental period, somatostatin was infused peripherally (0.8 μg · kg^{-1} · min^{-1}; Bachem, Torrance, CA) to inhibit the endocrine pancreas, and glucagon was replaced intraportally in basal amounts (0.57 ng · kg^{-1} · min^{-1}; Lilly, Indianapolis, IN). In the control group ($n = 7$), insulin (Lilly) was infused intraportally at rates matched to basal levels (240 μU · kg^{-1} · min^{-1}). In the experimental group ($n = 20$), insulin was infused intraportally at a rate (2,000 μU · kg^{-1} · min^{-1}) that produced an eightfold rise from baseline. In all studies, glucose was infused peripherally as required to maintain euglycemia. In the control group, subsets of experiments were terminated either after 2 h ($n = 4$) or 4 h ($n = 3$). In the experimental group, a subset of experiments were terminated after 0.5 h ($n = 5$), 1 h ($n = 4$), 2 h ($n = 6$), and 4 h ($n = 5$). Immediately after obtaining the final blood sample, each animal was anesthetized with pentobarbital and a laparotomy was performed. The hormone and glucose infusions were continued while liver sections from three separate lobes were freeze-clamped in situ and subsequently stored at −70°C. Liver biopsies were obtained within 3 min of the final blood sample time. Initial molecular analysis verified that there were minimal differences in cellular signals between lobes, and as a result, the molecular data reported for all animals were generated from analysis of liver lobe 2. There were no differences between markers assessed in control samples taken after 2 or 4 h of basal insulinemia; thus, the molecular data reported for the control group reflect pooled data from all control animals.

Metabolite analysis. Hematocrit levels, glucose, glucagon, insulin, cortisol, and nonesterified fatty acid (NEFA) levels in plasma and alanine, glycine, serine, threonine, lactate, glutamine, glutamate, glycerol, and β-hydroxybutyrate concentrations in blood were determined using standard procedures as previously described (5).

Molecular analysis. RNA extraction, cDNA synthesis, real-time PCR, SDS-PAGE, and Western blotting were performed using standard methods (17). Fructose-2,6-bisphosphate ($F2,6P_2$) concentration and enzyme activities of pyruvate kinase, G6Pase, glycogen synthase, and glycogen phosphorylase were assessed using established methods (18–22).

Preparation of monoacetone glucose and ^{2}H NMR (nuclear magnetic resonance) spectroscopy. Whole-body GNG and glycogenolysis were calculated using the ^2H_2O method combined with nuclear magnetic resonance (NMR) analysis as previously described (23). NMR spectra were generated independently for each animal. Briefly, 10-ml plasma samples were deproteinized and lyophilized. To convert plasma glucose to monoacetone glucose, the dried residue was suspended in 5.0 ml acetone containing 200 μl H_2SO_4. The suspension was mixed for 4 h at room temperature. After addition of 5 ml H_2O, pH was adjusted to 2 with drop-wise addition of 1.5 mol/l Na_2CO_3, and the sample was mixed for 24 h at room temperature. The pH was then further increased to 8 using Na_2CO_3, and the sample was dried. Monoacetone glucose was extracted (three to four times) by addition of 3 ml hot ethyl acetate. Ethyl

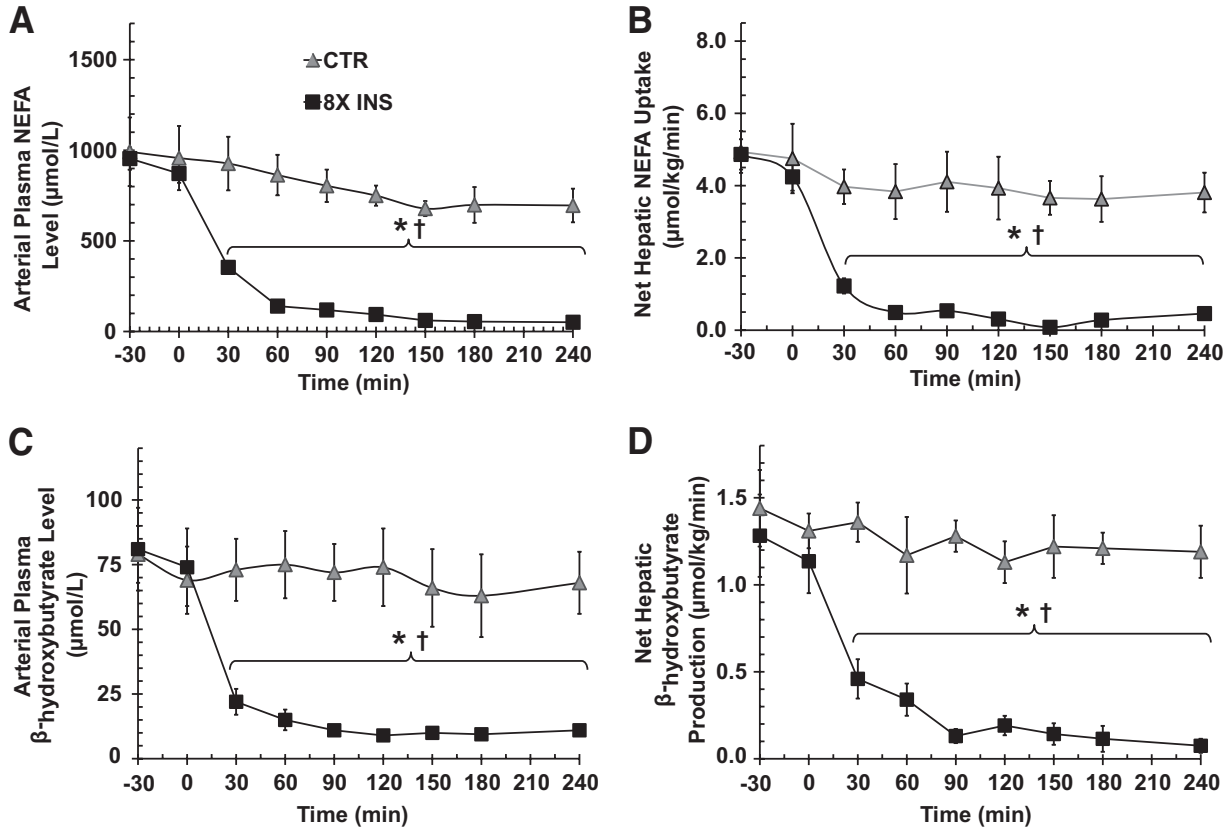

FIG. 2. Arterial plasma NEFA levels (*A*), net hepatic NEFA uptake (*B*), arterial plasma β-hydroxybutyrate levels (*C*), and net hepatic β-hydroxybutyrate production (*D*) in 24 h fasted conscious dogs during the basal (−30 to 0 min) and experimental (0–240 min) periods. Data are means ± SEM; $n = 7$ in control (CTR) and $n = 20$ in 8× insulin (8X INS) groups. *$P < 0.05$ vs. CTR group; †$P < 0.05$ vs. basal period.

acetate was removed via vacuum evaporation, and monoacetone glucose was further purified by passage through a solid-phase extraction tube using ethyl acetate as eluant. The effluent was freeze-dried and stored before NMR analysis.

NMR spectra for monoacetone glucose (dissolved in 100% acetonitrile) were acquired using a 14.0 T Bruker magnet equipped with a Bruker AV-III console operating at 92.12 MHz for ^{2}H. All spectra were acquired in 3-mm NMR tubes using a Bruker 5-mm TCI cryogenically cooled NMR probe. Chemical shifts were referenced internally to CD_3CN (1.98 ppm). For 1D ^{2}H NMR, typical experimental conditions included 2K data points, 20 ppm sweep width, a recycle delay of 0.5 s, and 12–25K scans, depending on sample concentration. Data were processed using TOPSPIN software provided by Bruker Biospin. Data analysis used an automated program for integration of the ^{2}H NMR spectra ensuring consistent and reproducible integration areas for all acquired spectra.

Calculations. We determined whole-body GNG and glycogenolysis using the following calculations: gluconeogenesis = $R_a \times$ C5/C2 and glycogenolysis = R_a − gluconeogenesis. R_a represents tracer-derived endogenous glucose production calculated using the two-compartment circulatory model described by Mari et al. (24), and C5/C2 represents the ratio of deuterium enrichment at the respective carbon positions of glucose.

Net hepatic substrate balances were calculated with the arterio-venous (A-V) difference method using the formula: net hepatic substrate balance = $Load_{out} - Load_{in}$, where $Load_{out} = [H] \times HF$ and $Load_{in} = [A] \times AF + [P] \times PF$. [A], [P], and [H] represent substrate concentrations in femoral artery, portal vein, and hepatic vein blood or plasma, respectively, and AF, PF, and HF represent blood or plasma flow (as measured using ultrasonic flow probes) through the hepatic artery, the portal vein, and the hepatic vein, respectively. With this calculation, positive values reflect net hepatic production and negative values represent net hepatic uptake. Plasma glucose values were multiplied by 0.73 to convert them to blood glucose values as previously validated (25). Net hepatic fractional extraction was calculated by dividing net hepatic substrate balance by hepatic substrate load. The approximate insulin and glucose levels in plasma entering the liver sinusoids were calculated using the formula [A] × %AF + [P] × %PF, where [A] and [P] represent arterial and portal vein concentrations, respectively, and %AF and %PF are the respective fractional contributions of arterial and portal blood flow to total hepatic blood flow.

We estimated net hepatic gluconeogenic (NHGNG) flux by subtracting glycolytic flux from gluconeogenic flux-to-G6P. GNG flux-to-G6P was determined by taking the sum of net hepatic uptake rates of gluconeogenic precursors (alanine, glycine, serine, threonine, glutamine, glutamate, glycerol, lactate, and pyruvate) and dividing by 2 to account for the incorporation of two three-carbon precursors into one six-carbon glucose molecule. Glycolytic flux was estimated by taking the sum of the net hepatic output rates (when present) of the gluconeogenic substrates noted above (in glucose equivalents) and hepatic glucose oxidation (assumed to be 0.2 ± 0.1 mg · kg^{-1} · min^{-1}). We have verified that glucose oxidation remains at a low and constant rate across wide variations in physiological parameters (26,27). Positive NHGNG flux reflects net GNG flux-to-G6P, whereas negative values represent net glycolytic flux to CO_2 or lactate. Net hepatic glycogenolytic flux was estimated by subtracting NHGNG flux from net hepatic glucose balance. Positive net hepatic glycogenolytic flux reflects net glycogen breakdown, and negative values represent net glycogen synthesis.

There are several assumptions required when using the A-V difference technique in assessment of GNG flux-to-G6P. For example, this method assumes that substrate flux is unidirectional at any given point in time. There is negligible production of gluconeogenic amino acids or glycerol by the liver, so for these substrates, the compromise is of little consequence. Predominantly gluconeogenic periportal and glycolytic perivenous hepatocytes could simultaneously take up and release lactate, respectively, which could lead to an underestimation of GNG flux-to-G6P. It must be noted that simultaneous lactate uptake and release would not, however, affect our estimation of NHGNG flux or net hepatic glycogenolytic flux. NHGNG flux and net hepatic glycogenolytic flux estimations are subject to error to the degree that intrahepatic GNG amino acids contribute to the formation of G6P. The method also assumes 100% conversion of the GNG amino acids taken up by the liver into G6P (they are not oxidized or used in the synthesis of proteins). Errors arising from the assumptions are difficult to assess but appear to be minimal, as simultaneous assessment of GNG flux using the A-V difference technique and other independent methods (that are not subject to the same assumptions) yielded similar estimates of GNG flux (5,28).

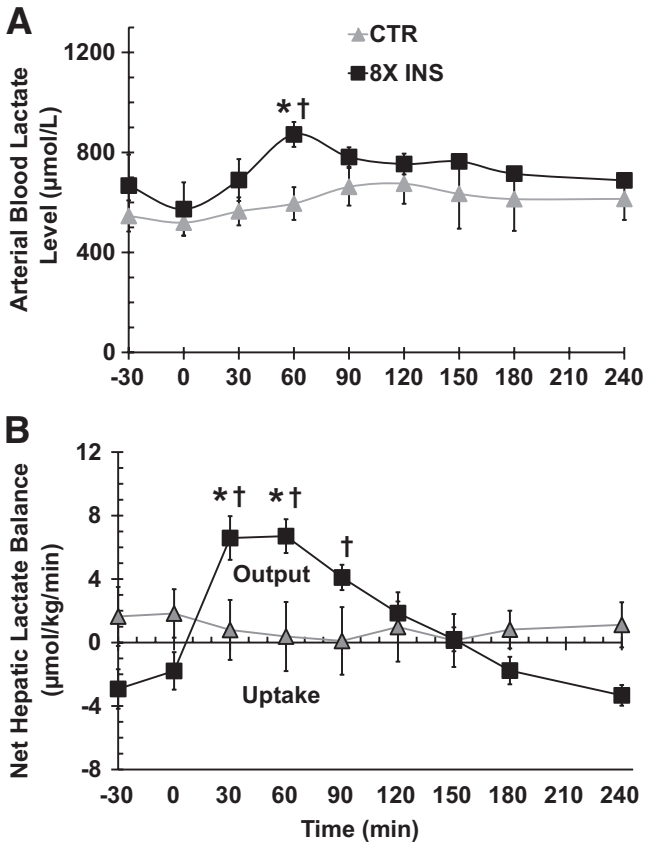

FIG. 3. Arterial blood lactate concentrations (*A*) and net hepatic lactate uptake (*B*) in 24 h fasted conscious dogs during the basal (−30 to 0 min) and experimental (0–240 min) periods. Data are means ± SEM; $n = 7$ in control (CTR) and $n = 20$ in 8× insulin (8X INS) groups. *$P < 0.05$ vs. CTR group; †$P < 0.05$ vs. basal period.

Statistical analysis. Statistical comparisons were carried out using two-way repeated-measure ANOVA (group × time) (SigmaStat). One-way ANOVA comparison tests were used post hoc when significant *F* ratios were obtained. Significance was determined as $P < 0.05$.

RESULTS

Hormone levels. In the control group, insulin was replaced at basal levels, whereas both arterial and hepatic sinusoidal insulin levels increased eightfold in the experimental group (Fig. 1*A* and *B*). Arterial and hepatic sinusoidal glucagon levels were clamped at basal values in all animals (Fig. 1*C* and *D*). Arterial cortisol levels were also basal in all animals (data not shown).

Fat metabolism. Arterial NEFA levels tended to decline slowly in the control group, resulting in a modest reduction by 240 min (Fig. 2*A*). Conversely, there was a rapid and marked decrease in arterial NEFA levels (61 and 96% at 30 and 240 min, respectively) in response to hyperinsulinemia. Consistent with these data, there were minimal changes in net hepatic NEFA uptake (Fig. 2*B*) and oxidation (Fig. 2*D*) in control animals, but rapid and substantial suppression of these parameters in the hyperinsulinemic group.

Gluconeogenic precursor metabolism. In control animals, there was no significant change in arterial blood lactate levels (Fig. 3*A*) or net hepatic lactate balance (Fig. 3*B*) over time. Conversely, hyperinsulinemia caused a transient increase in arterial blood lactate levels and a switch from net hepatic lactate uptake to net hepatic lactate output that was evident between 30 and 120 min. By 240 min, net hepatic lactate uptake had returned to baseline rates.

While arterial plasma glycerol levels and net hepatic glycerol uptake did not change significantly in the control group, both of these parameters decreased rapidly (50 and 61% by 30 min) in response to hyperinsulinemia and remained suppressed for the duration of the study (supplementary Table 1, which can be found in an online appendix at http://diabetes.diabetesjournals.org/cgi/content/full/db09-1625/DC1). There were no significant changes over time in arterial blood alanine levels, net hepatic fractional extraction of alanine, or net hepatic alanine balance in the control group (supplementary Table 1). Conversely, blood alanine concentrations eventually fell (40 and 54% by 120 and 240 min, respectively) in response to hyperinsulinemia. Net hepatic alanine uptake rates did not change over time in the hyperinsulinemic group despite the decreased arterial levels because net hepatic fractional extraction of alanine increased (1.8-fold by 240 min). Similar trends were observed for serine, glycine, threonine, glutamate, and glutamine (data not shown). Thus, in the control animals, the summed blood level, net hepatic fractional extraction, and net hepatic uptake of gluconeogenic amino acids failed to change. Hyperinsulinemia, on the other hand, resulted in a gradual decrease in amino acid levels in blood (32% after 240 min), an increase (56% by 240 min) in their net hepatic fractional extraction, and no change in their net hepatic uptake (supplementary Table 1).

Glucose, glycogenolytic, and gluceoneogenic flux rates. Euglycemia was maintained in all animals (Fig. 4*A*), requiring glucose infusion rates of 0.2 ± 0.1 and 13.3 ± 0.9 $mg \cdot kg^{-1} \cdot min^{-1}$ in the control and hyperinsulinemic groups, respectively, during the last hour of study. In the basal period, net hepatic glucose output was similar (2.0 $mg \cdot kg^{-1} \cdot min^{-1}$) in both groups. Net hepatic glucose output declined minimally (17%) over time in the control group (Fig. 4*B*), whereas in the hyperinsulinemic group, it rapidly declined (75% by 30 min) and was completely inhibited by 60 min, after which the liver switched to net glucose uptake (0.8 ± 0.1 $mg \cdot kg^{-1} \cdot min^{-1}$ at 240 min). Net hepatic glycogenolytic flux fell slightly (~25%, NS) over time in the control group but was rapidly suppressed (43% reduction by 30 min) by hyperinsulinemia, being completely inhibited by 60 min. By the end of the study, the liver had switched to a state of net hepatic glycogen synthesis (Fig. 4*C*). NHGNG flux did not change from basal in the control group but was transiently decreased in response to hyperinsulinemia so that the liver switched to net glycolysis from 30 to 90 min (Fig. 4*D*). By the end of the study, NHGNG flux had returned to near-basal. The suppression of net hepatic glucose output by hyperinsulinemia was confirmed by reduced tracer-derived endogenous glucose production (Fig. 5*A*) and was indicative of the complete suppression (at 240 min) of whole-body GNG (Fig. 5*B*) and glycogenolysis (Fig. 5*C*), as determined using the ^2H_2O technique.

Molecular effects of insulin. The time course of intracellular insulin-regulated events was assessed in hepatic biopsies obtained from the hyperinsulinemic group and expressed relative to the data obtained from control animals. In response to hyperinsulinemia, Akt and GSK-3β phosphorylation increased approximately twofold and approximately threefold at 30 and 60 min, respectively, relative to the control group (Fig. 6*A*). The level of

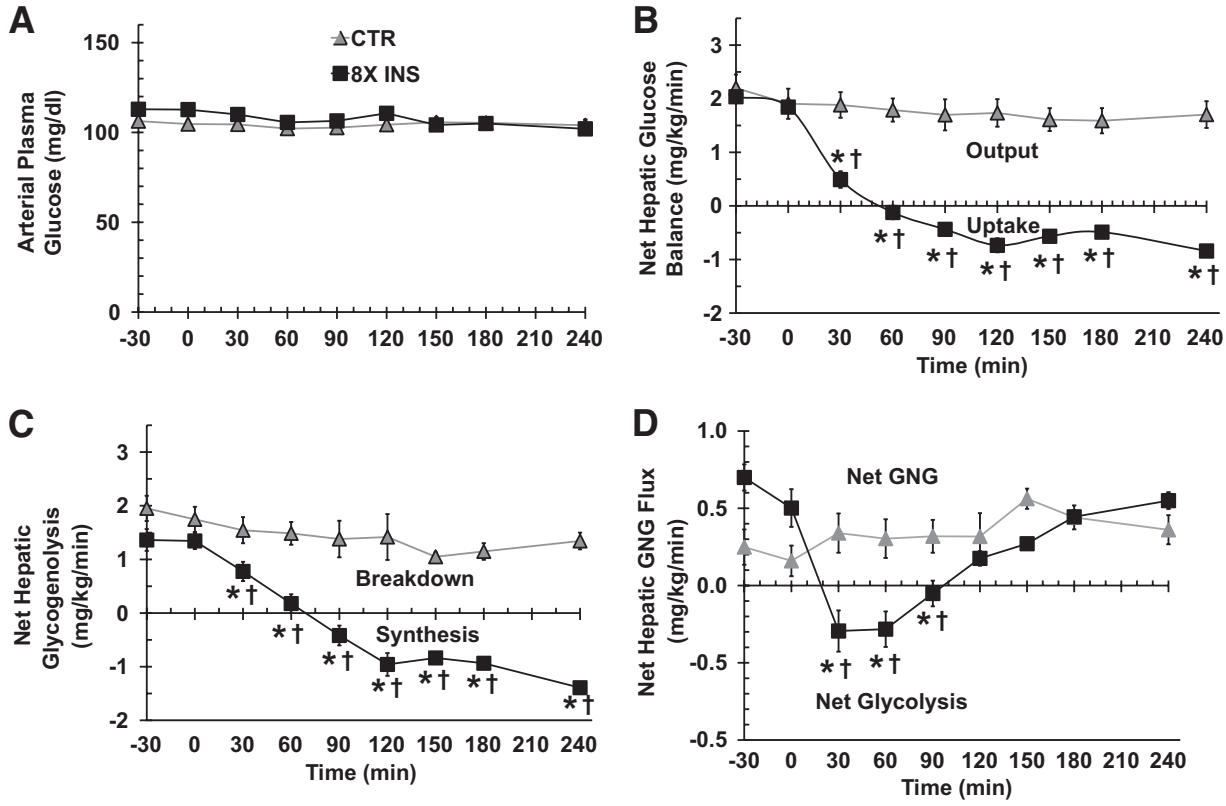

FIG. 4. Arterial plasma glucose levels (*A*), net hepatic glucose balance (*B*), net hepatic glycogenolytic flux (*C*), and net hepatic gluconeogenic flux (*D*) in 24 h fasted conscious dogs during the basal (−30 to 0 min) and experimental (0–240 min) periods. Data are means ± SEM; $n = 7$ in CTR and $n = 20$ in 8× insulin (8X INS) groups. *$P < 0.05$ vs. CTR group; †$P < 0.05$ vs. basal period.

phosphorylated glycogen synthase tended to decrease (~20%, NS) by 60 min and was maximally reduced (45%) for the last 120 min of the study (Fig. 6*B*). The glycogen synthase activity ratio was elevated twofold from 30 min on (Fig. 6*C*), whereas the glycogen phosphorylase activity ratio was decreased 40% (Fig. 6*D*).

Hyperinsulinemia caused a twofold increase in FOXO1 phosphorylation (and 52% decrease in nuclear FOXO1 content) by 30 min (Fig. 7*A*). FOXO1 levels in nuclear-enriched fractions eventually decreased by 95% in the hyperinsulinemic group. CRTC2 phosphorylation increased approximately twofold, and PGC1α protein levels decreased (43%) by 120 min (Fig. 7*B*). STAT3 phosphorylation increased approximately twofold, but it took 240 min before a significant change was observed (Fig. 7*C*). Hyperinsulinemia resulted in rapid (45–50% by 30 min) and marked (80–90% by 240 min) decreases in PEPCK and G6Pase mRNA (Fig. 7*D*). The PEPCK protein level did not change during the first hour of hyperinsulinemia but was reduced 31 and 48% at 120 and 240 min, respectively (Fig. 7*E*), whereas G6Pase activity was modestly reduced at 240 min (~30%, NS, Fig. 7*F*).

Glucokinase opposes the action of G6Pase. Hyperinsulinemia stimulated 3- and 11-fold increases in glucokinase mRNA at 30 and 240 min, respectively, whereas glucokinase protein was not elevated until 120 min (twofold) and was elevated threefold by 240 min (Fig. 8*A*). Hepatic $F2,6P_2$ concentration and pyruvate kinase activity, both of which stimulate glycolysis and inhibit GNG, were also assessed. $F2,6P_2$ increased approximately threefold by 30 min and fivefold by 60 min in response to hyperinsulinemia and remained elevated for the duration of the experiment (Fig. 8*B*). Pyruvate kinase activity was increased 1.7-fold for the last 120 min of hyperinsulinemia (Fig. 8*C*).

DISCUSSION

The distinction between hepatic gluconeogenesis (GNG; liver production of glucose derived from GNG precursors) and gluconeogenic formation of G6P is crucial to the interpretation of insulin's effect on HGP. In the present study, a physiological eightfold rise in portally infused insulin rapidly inhibited HGP in 24 h fasted dogs. Thus, glycogenolysis and gluconeogenesis, classically defined as hepatic output of glucose derived from the glycogenolytic and gluconeogenic pathways, were both sharply reduced. However, the inhibition of NHGNG flux was transient, so that after 240 min, it was unchanged from baseline. Thus, by the end of the study, insulin had reduced the GNG fraction of HGP to zero without affecting the net gluconeogenic rate of G6P formation, but rather by promoting the deposition of G6P in glycogen. Net hepatic glycogenolytic flux was strongly inhibited by 30 min and completely suppressed by 60 min, and thereafter the liver exhibited net glycogen synthesis. The metabolic conversion of the liver to an organ of net glycogen storage correlated with insulin's rapid and reciprocal regulation of glycogen phosphorylase (↓) and glycogen synthase (↑). Insulin eventually (120 min) brought about an increase in glucokinase protein and thus glucokinase may have played a role in facilitating glucose entry and in sustaining the maximal rate of glycogen synthesis.

Hyperinsulinemia resulted in substantial decreases (40–50%) in PEPCK and G6Pase mRNA at 30 min, which

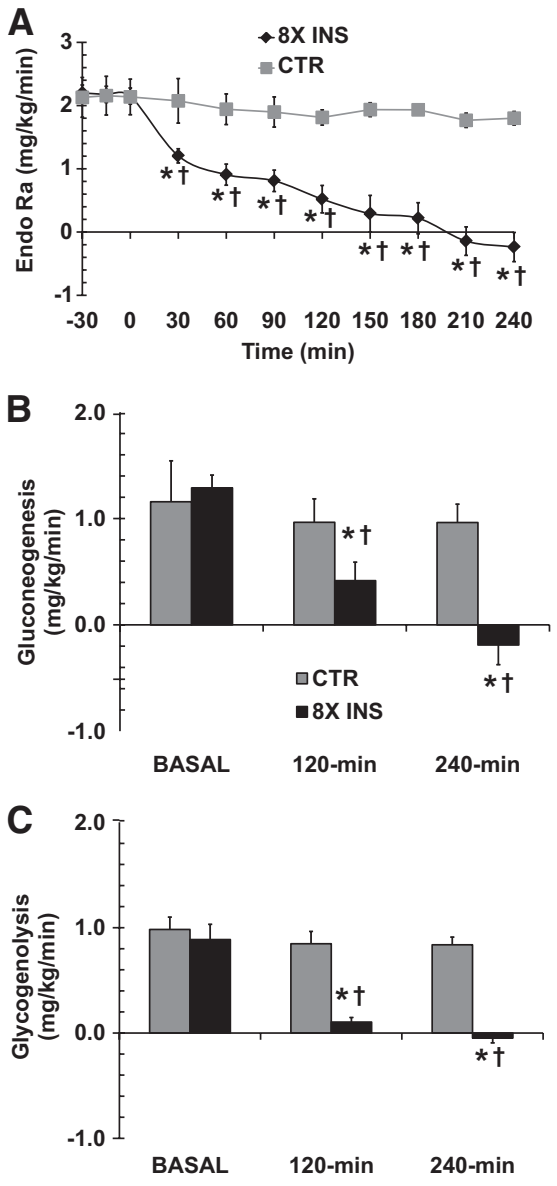

FIG. 5. Tracer-determined endogenous glucose production (*A*), whole-body gluconeogenesis (*B*), and whole-body glycogenolysis (*C*) determined using the ^2H_2O method in 24 h fasted conscious dogs during the basal (−30 to 0 min) and experimental (0–240 min) periods. Deuterated water analysis was performed on subsets of control (CTR) and hyperinsulinemic experiments that were carried out for 240 min (n = 3 and n = 5, respectively). Data represent means ± SEM; *P < 0.05 vs. CTR group, †P < 0.05 vs. basal period. 8X INS, 8× insulin.

correlated with the time course of FOXO1 phosphorylation and preceded changes in other key regulatory loci (CRTC2, PGC1α, STAT3). PEPCK mRNA was suppressed by >80% at 2 h, before any significant increases in STAT3 phosphorylation. STAT3 inhibits GNG mRNA expression (29), and in mice, it has been suggested that STAT3 is the hepatic effector for insulin-brain-liver signaling required for suppression of GNG in vivo (13). Regardless of the validity of this concept, which is doubted by some (30), we show here that the repression of GNG mRNA expression is associated with FOXO1 phosphorylation and occurs before STAT3-mediated regulation.

While we verified that the rodent-derived model of insulin-mediated suppression of GNG gene expression is intact and applicable to large animals, these molecular events did not affect the acute regulation of NHGNG flux. Hyperinsulinemia reduced NHGNG flux (resulting in net glycolysis) at 30 min, and this preceded functional changes in gluconeogenic enzymes (PEPCK, G6Pase) or the activation of pyruvate kinase, which is considered to be a key regulatory enzyme of glycolysis (31). On the other hand, it correlated with an increase in hepatic $F2,6P_2$ and a decrease in lipolysis and hepatic fat oxidation. This suggests that hepatic $F2,6P_2$ and hepatic fat oxidation have greater regulatory strength over the insulin-mediated enhancement of glycolysis in vivo than does pyruvate kinase. Insulin stimulates the dephosphorylation of 6-phosphofructokinase-2 (PFK-2)/fructose-2,6-bisphosphatase (FBPase-2), increasing PFK-2 activity and inhibiting FBPase-2 activity, the net of which increases the level of $F2,6P_2$, a metabolite that promotes glycolysis and inhibits GNG in vitro (31). Oxidation of fat by the liver generates intrahepatic metabolites that inhibit glycolysis and promote GNG. Insulin-mediated suppression of lipolysis therefore results in the removal of these cues (32). Indeed, after 30 min, glycolysis was enhanced and glycogenolytically derived carbon entered glycolysis and exited the liver in the form of lactate rather than glucose. As a consequence, the liver switched from a state of net lactate consumption (using lactate as a GNG precursor) to an organ of net lactate production.

We previously observed that selective peripheral hyperinsulinemia (with no change in insulin at the liver or, presumably, $F2,6P_2$) suppressed HGP due to a reduction in NHGNG flux, and the time course of this suppression correlated with decreased lipolysis and increased net hepatic lactate output (33). When arterial NEFA levels were clamped at basal levels with intralipid infusion, peripheral hyperinsulinemia could not modify hepatic glycolysis, net hepatic lactate balance, or NHGNG flux (33). In another study, selective hepatic hyperinsulinemia (and, presumably, increased $F2,6P_2$, with no change in arterial insulin) suppressed HGP entirely by inhibiting glycogenolysis, without altering NHGNG flux (34). Taken together, these studies (33,34) suggest that acute regulation of NHGNG flux by insulin is caused by the suppression of lipolysis and may be independent of changes in $F2,6P_2$. It must be noted that $F2,6P_2$ was not assessed in these earlier studies (33,34), whereas it was in the present study, so we cannot be certain which (increased $F2,6P_2$ or decreased lipolysis) was the dominant factor mediating the transient decrease in NHGNG flux.

By 240 min, NHGNG flux had returned to its baseline value despite an ~50% reduction in PEPCK protein and persisting conditions that favored glycolysis (increased $F2,6P_2$, increased pyruvate kinase activity, and decreased hepatic fat oxidation). Theoretically, the transient decrease in NHGNG could have reflected enhanced glycolytic flux, decreased GNG flux-to-G6P, or both. Our observation that GNG flux-to-G6P was basal at 240 min suggests that the transient change in NHGNG flux was due to an alteration in glycolysis (supplementary Fig. 1). GNG flux-to-G6P remains active and important to glycogen deposition in the postprandial state in a variety of species, suggesting that the pathway is insensitive to hyperinsulinemia (and insulin-mediated increased $F2,6P_2$) in vivo (35–39). Conversely, hyperinsulinemia (and the resulting increased $F2,6P_2$) has been shown to enhance glycolysis in vivo, and this has been suggested to be a mechanism by which insulin reduces HGP (40–42). The rebound in NHGNG flux likely resulted from the cessation of glycogen

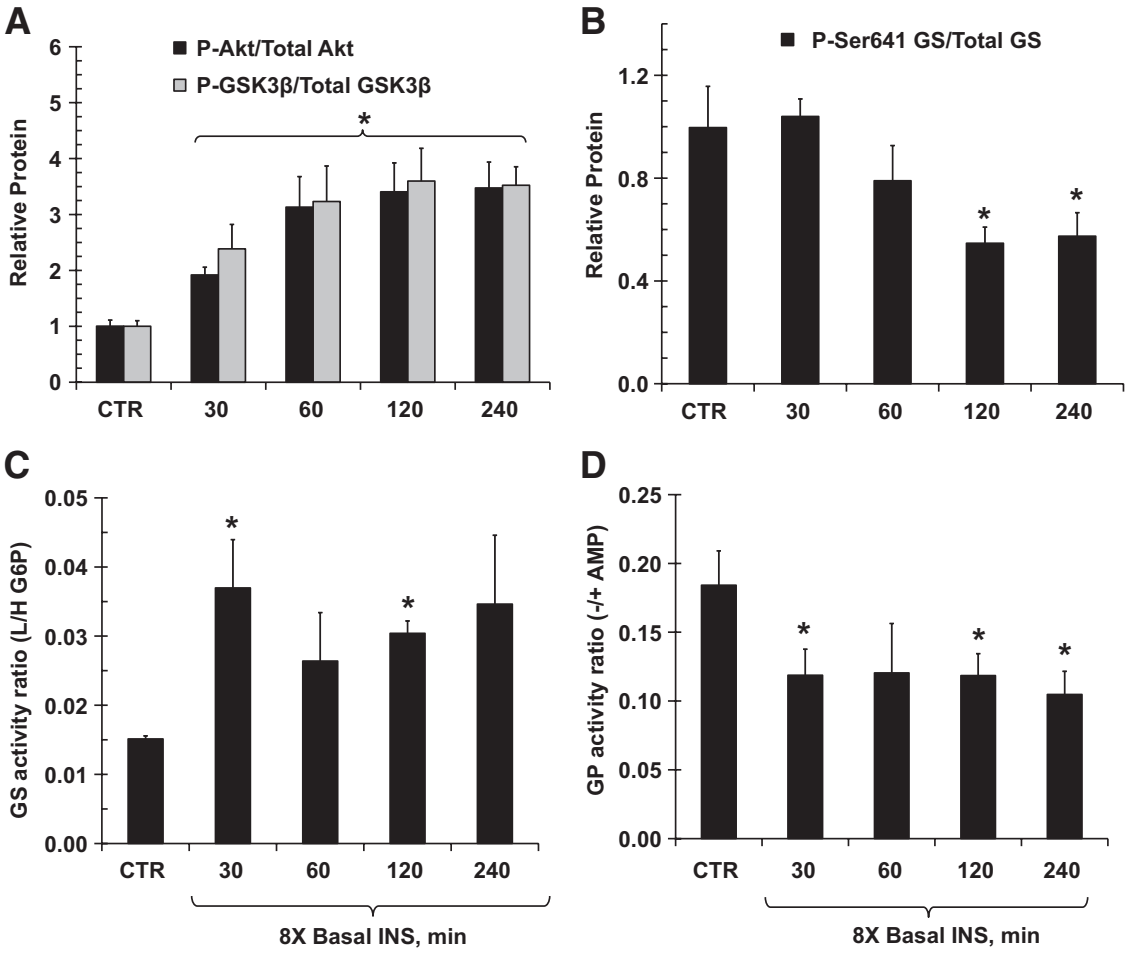

FIG. 6. Molecular regulation of glycogen metabolism in 24 h fasted conscious dogs after either CTR or 8X INS treatments. *A*: Akt and GSK3β phosphorylation, expressed relative to total Akt and GSK3β protein content, respectively. *B*: Phosphorylation of glycogen synthase, expressed relative to total glycogen synthase. *C*: Glycogen synthase activity ratio (independent versus total, measured using 0.1 vs. 10 mmol/l G6P, respectively). *D*: Glycogen phosphorylase activity ratio (independent versus total, measured in the absence versus presence [3 mmol/l] of AMP, respectively). Histograms depict mean values ± SEM. *Significantly different from the value for control (CTR), $P < 0.05$. 8X INS, 8× insulin.

breakdown and the reduction in substrate for the glycolytic pathway. This, in turn, caused the restoration of net hepatic lactate uptake and the deposition of gluconeogenically derived carbon in glycogen. Thus, the complete suppression of HGP observed after several hours of hyperinsulinemia appears to have been a function of the switch from net glycogenolysis to net glycogen synthesis, with NHGNG flux being unchanged.

The notion that insulin can inhibit GNG flux-to-G6P is based largely on experiments carried out using isolated hepatocytes and perfused livers from rats (31). However, these studies typically examined the process in the absence of many factors (hepatic glycogen, neural input, and physiological concentrations of other hormones and circulating fatty acids) that play important roles in the regulation of HGP in vivo (16). For example, in mice, the deletion of CRTC2 resulted in reduced PEPCK and G6Pase gene expression in vitro and in vivo; however, while this impaired glucagon-stimulated HGP in vitro, it did not alter glucose metabolism in vivo (43). Additionally, insulin-induced inhibition of glucose output from liver tissue in vitro could reflect changes in glycogen synthesis and glycolysis, as well as alteration in GNG flux-to-G6P. Thus, in vitro studies of GNG are limited in their ability to characterize the physiologic regulation of the pathway in vivo.

Based on recent rodent studies, it was concluded that hyperinsulinemia in the brain inhibited HGP by reducing GNG associated with inhibition of GNG gene expression (13–15) and STAT3 phosphorylation (13). It is possible that the sensitivity and mechanism of insulin-mediated inhibition of HGP may be species-dependent. Rodents have 5–10× the basal HGP rates of large animals, and they exhaust liver glycogen stores after a fairly short fast, whereas canines (and humans) have the capacity to maintain a significant amount of liver glycogen after several days of fasting (44,45). It is also possible that the drive to maintain GNG flux-to-G6P during hyperinsulinemia differs between species. However, certain rodent studies have shown that GNG flux-to-G6P persists (with carbon redirected to glycogen) during feeding (37,38), which contradicts the notion that hyperinsulinemia can inhibit the pathway. The sensitivity of GNG flux-to-G6P to insulin may also vary according to dose and fasting length; we recently reported that ~16-fold hyperinsulinemia could suppress GNG flux-to-G6P in prolonged fasted (60 h) dogs in a manner that could not be explained by functional changes in PEPCK (17). Thus, there is uncertainty regarding the physiological and experimental circumstances under which insulin-mediated suppression of GNG flux-to-G6P can be detected.

Several early studies in rats showed that selective

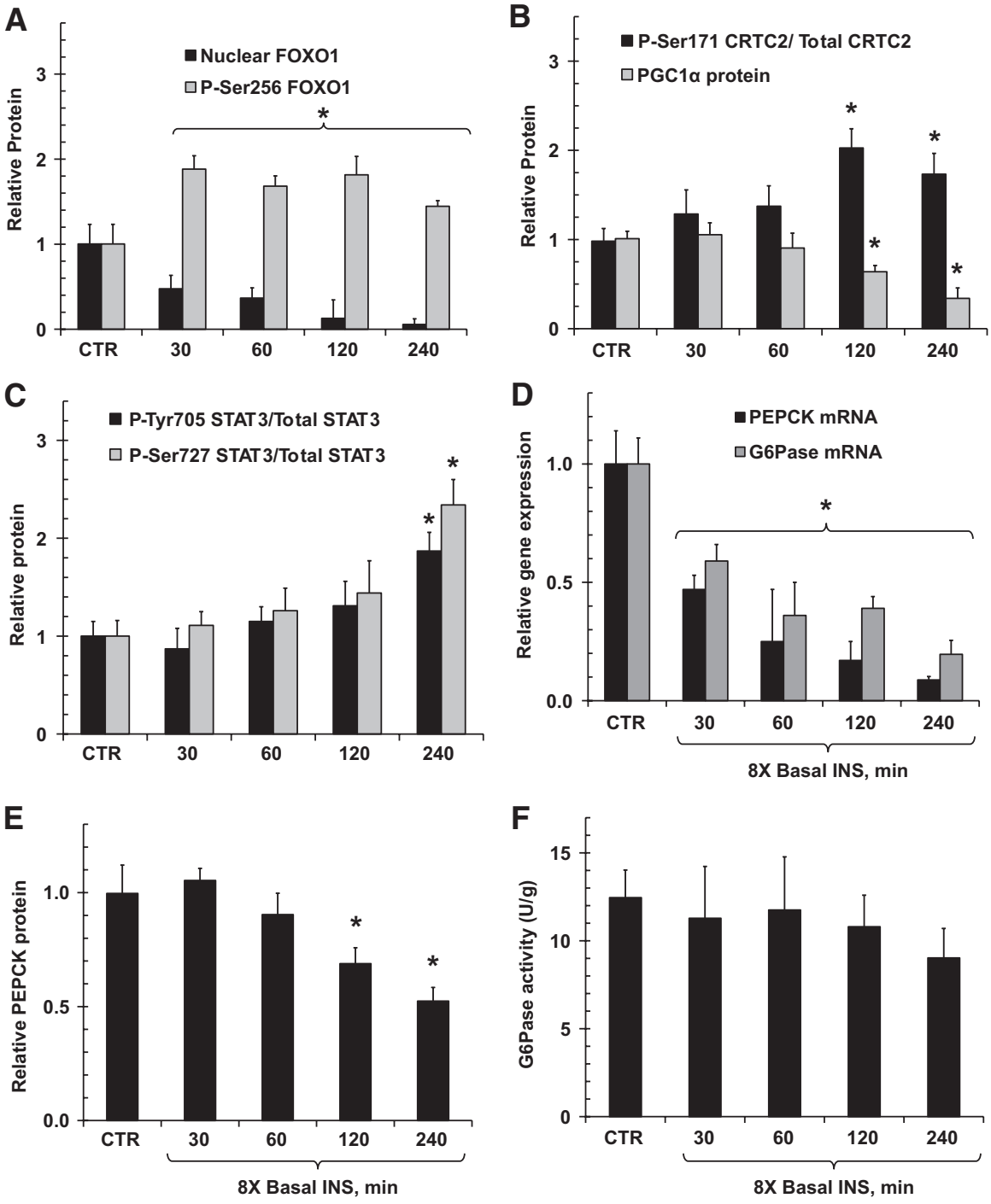

FIG. 7. Molecular regulation of GNG in 24 h fasted conscious dogs after either control (CTR) or 8× insulin (8X INS) treatments. *A*: FOXO1 phosphorylation and relative FOXO1 abundance in nuclear extracts. *B*: CRTC2 phosphorylation relative to CRTC2 total protein and PGC1α protein levels. *C*: STAT3 phosphorylation expressed relative to total STAT3 protein. *D*: Relative mRNA levels of PEPCK and G6Pase. *E*: PEPCK protein levels. *F*: G6Pase activity levels. Histograms depict mean values ± SEM. *Significantly different from the value for CTR, $P < 0.05$.

pharmacological inhibition (with 3-mercaptopicolinate) of PEPCK reduced GNG from gluconeogenesis precursors in vitro and lowered blood glucose and the GNG fraction of glycogen formation in vivo (38,46–48). These studies led to the notion that PEPCK is a dominant point of control in regulating GNG. However, these rat data may not be entirely transferable to humans due to the aforementioned differences between species. Furthermore, the complete inhibition of PEPCK activity achieved with 3-mercaptopicolinate is different from physiological inhibition of PEPCK protein by insulin, which, even after 4 h in our study, only reduced the protein by ~50%. This distinction is supported by a recent study using perfused livers from transgenic mice with large variations in hepatic PEPCK enzyme (49). Data from Burgess et al. (49) demonstrated that a 50% reduction in PEPCK protein content was not associated with a significant decrease in flux through PEPCK, whereas the complete absence of PEPCK protein did inhibit the pathway. Thus, our data support the notion that, under physio-

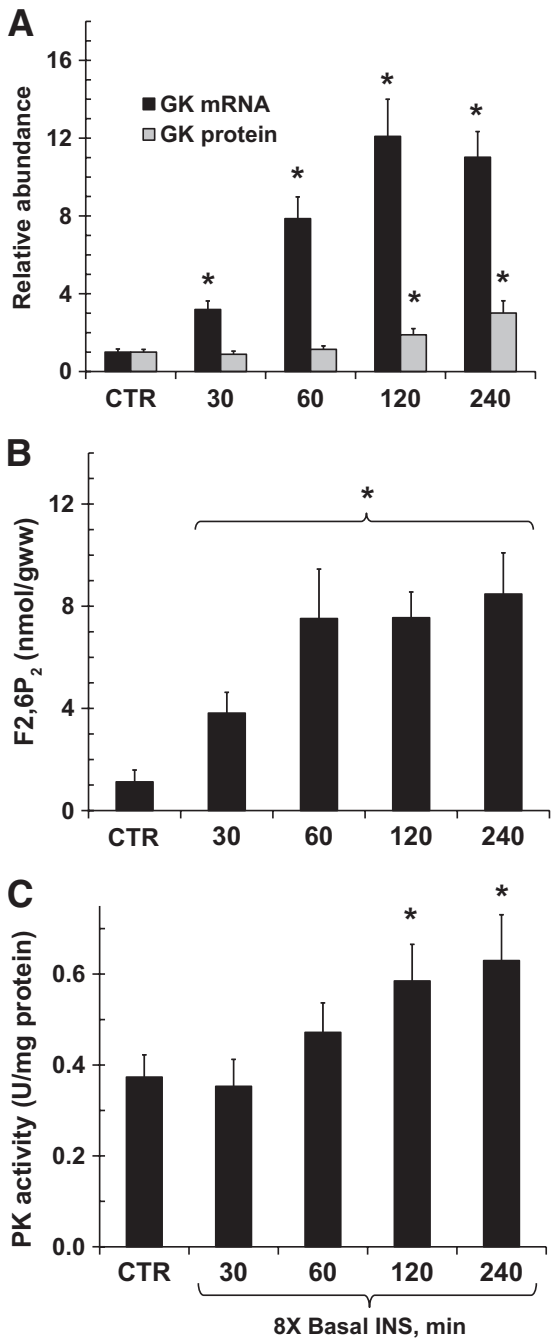

FIG. 8. *A*: Relative glucokinase (GK) mRNA expression and protein levels. *B*: Hepatic levels of F2,6P_2 (expressed per gram wet weight, gww). *C*: Hepatic pyruvate kinase (PK) activity. Histograms depict mean values ± SEM. *Significantly different from the value for CTR, $P < 0.05$.

logical circumstances in vivo, PEPCK has low control strength over the process (49).

It is possible that GNG enzyme activity may exert a higher degree of control on GNG in a chronic insulin-resistant state, since rodent models of diabetes typically display elevated HGP associated with increased PEPCK and G6Pase mRNA (50–52). However, Samuel et al. (53) recently showed that HGP and GNG were increased in two rodent models of diabetes despite normal levels of hepatic GNG enzyme mRNA. Furthermore, this group verified that PEPCK and G6Pase mRNA levels were not increased in human liver biopsies obtained from individuals with type 2 diabetes. While PEPCK may have high control strength on other aspects of hepatic metabolism such as TCA cycle flux (49), the notion that PEPCK is rate-determining in the GNG process appears to be inaccurate.

In summary, physiological hyperinsulinemia rapidly suppressed HGP in the conscious dog, and after 4 h, this inhibition was solely due to profound effects on glycogen metabolism with no alteration in NHGNG or GNG flux-to-G6P. Canonical insulin-mediated signaling mechanisms were rapidly activated, and the switch from glycogenolysis to glycogen synthesis was associated with the activation of glycogen synthase and inhibition of glycogen phosphorylase. Hyperinsulinemia led to the phosphorylation of FOXO1 and suppression of PEPCK and G6Pase mRNA levels, before alterations in other regulatory loci (CRTC2/PGC1α/STAT3). By 30 min, insulin increased hepatic F2,6P_2 and decreased hepatic fatty acid oxidation; these factors stimulated glycolysis, resulting in net lactate production and a transient reduction in NHGNG flux. NHGNG flux returned to baseline (despite substantially reduced PEPCK protein) by the end of the study as carbon was redirected to glycogen synthesis. We conclude that acute hyperinsulinemia regulates HGP through transient alterations in glycolysis and persisting effects on glycogen metabolism. Physiologic hyperinsulinemia has little or no effect on gluconeogenic formation of G6P despite reduced levels of PEPCK protein, indicating that PEPCK has little control over the gluconeogenic pathway.

ACKNOWLEDGMENTS

This research was supported in part by National Institutes of Health Grant R37-DK-18243 and the Diabetes Research and Training Center Grant SP-60-AM20593. C.J.R. was supported by an American Diabetes Association mentor-based fellowship. A.D.C. was supported by the Jacquelyn A. Turner and Dr. Dorothy J. Turner Chair in Diabetes Research.

No other potential conflicts of interest relevant to this article were reported.

We thank Dr. Masakazu Shiota, Dr. Rob Hall, Jon Hastings, Angelina Penaloza, Wanda Snead, Patrick Donahue, and Suzan Vaughan (Vanderbilt University) for their excellent technical support. We are grateful to Dr. Alex Lange (University of Minnesota) for providing reagents and expertise.

REFERENCES

1. Adkins A, Basu R, Persson M, Dicke B, Shah P, Vella A, Schwenk WF, Rizza R. Higher insulin concentrations are required to suppress gluconeogenesis than glycogenolysis in nondiabetic humans. Diabetes 2003;52:2213–2220
2. Boden G, Cheung P, Homko C. Effects of acute insulin excess and deficiency on gluconeogenesis and glycogenolysis in type 1 diabetes. Diabetes 2003;52:133–137
3. Boden G, Cheung P, Stein TP, Kresge K, Mozzoli M. FFA cause hepatic insulin resistance by inhibiting insulin suppression of glycogenolysis. Am J Physiol Endocrinol Metab 2002;283:E12–E19
4. Cherrington AD. Banting Lecture 1997. Control of glucose uptake and release by the liver in vivo. Diabetes 1999;48:1198–1214
5. Edgerton DS, Cardin S, Emshwiller M, Neal D, Chandramouli V, Schumann WC, Landau BR, Rossetti L, Cherrington AD. Small increases in insulin inhibit hepatic glucose production solely caused by an effect on glycogen metabolism. Diabetes 2001;50:1872–1882
6. Gastaldelli A, Toschi E, Pettiti M, Frascerra S, Quiñones-Galvan A, Sironi AM, Natali A, Ferrannini E. Effect of physiological hyperinsulinemia on gluconeogenesis in nondiabetic subjects and in type 2 diabetic patients. Diabetes 2001;50:1807–1812
7. Nuttall FQ, Ngo A, Gannon MC. Regulation of hepatic glucose production

and the role of gluconeogenesis in humans: is the rate of gluconeogenesis constant? Diabete Metab Res Rev 2008;24:438–458
8. Petersen KF, Laurent D, Rothman DL, Cline GW, Shulman GI. Mechanism by which glucose and insulin inhibit net hepatic glycogenolysis in humans. J Clin Invest 1998;101:1203–1209
9. Villar-Palasí C, Guinovart JJ. The role of glucose 6-phosphate in the control of glycogen synthase. FASEB J 1997;11:544–558
10. Liu Y, Dentin R, Chen D, Hedrick S, Ravnskjaer K, Schenk S, Milne J, Meyers DJ, Cole P, Yates J 3rd, Olefsky J, Guarente L, Montminy M. A fasting inducible switch modulates gluconeogenesis via activator/coactivator exchange. Nature 2008;456:269–273
11. Puigserver P, Rhee J, Donovan J, Walkey CJ, Yoon JC, Oriente F, Kitamura Y, Altomonte J, Dong H, Accili D, Spiegelman BM. Insulin-regulated hepatic gluconeogenesis through FOXO1-PGC-1alpha interaction. Nature 2003;423:550–555
12. Schilling MM, Oeser JK, Boustead JN, Flemming BP, O'Brien RM. Gluconeogenesis: re-evaluating the FOXO1-PGC-1alpha connection. Nature 2006; 443:E10–E11
13. Inoue H, Ogawa W, Asakawa A, Okamoto Y, Nishizawa A, Matsumoto M, Teshigawara K, Matsuki Y, Watanabe E, Hiramatsu R, Notohara K, Katayose K, Okamura H, Kahn CR, Noda T, Takeda K, Akira S, Inui A, Kasuga M. Role of hepatic STAT3 in brain-insulin action on hepatic glucose production. Cell Metab 2006;3:267–275
14. Obici S, Zhang BB, Karkanias G, Rossetti L. Hypothalamic insulin signaling is required for inhibition of glucose production. Nat Med 2002;8:1376–1382
15. Pocai A, Lam TK, Gutierrez-Juarez R, Obici S, Schwartz GJ, Bryan J, Aguilar-Bryan L, Rossetti L. Hypothalamic K(ATP) channels control hepatic glucose production. Nature 2005;434:1026–1031
16. Cherrington AD, Moore MC, Sindelar DK, Edgerton DS. Insulin action on the liver in vivo. Biochem Soc Trans 2007;35:1171–1174
17. Edgerton DS, Ramnanan CJ, Grueter CA, Johnson KM, Lautz M, Neal DW, Williams PE, Cherrington AD. Effects of insulin on the metabolic control of hepatic gluconeogenesis in vivo. Diabetes 2009;58:2766–2775
18. Arion WJ. Measurement of intactness of rat liver endoplasmic reticulum. Methods Enzymol 1989;174:58–67
19. Guinovart JJ, Salavert A, Massagué J, Ciudad CJ, Salsas E, Itarte E. Glycogen synthase: a new activity ratio assay expressing a high sensitivity to the phosphorylation state. FEBS Lett 1979;106:284–288
20. Storey KB. Regulation of liver metabolism by enzyme phosphorylation during mammalian hibernation. J Biol Chem 1987;262:1670–1673
21. Thomas JA, Schlender KK, Larner J. A rapid filter paper assay for UDPglucose-glycogen glucosyltransferase, including an improved biosynthesis of UDP-14C-glucose. Anal Biochem 1968;25:486–499
22. Wu C, Khan SA, Peng LJ, Lange AJ. Roles for fructose-2,6-bisphosphate in the control of fuel metabolism: beyond its allosteric effects on glycolytic and gluconeogenic enzymes. Adv Enzyme Regul 2006;46:72–88
23. Burgess SC, Hausler N, Merritt M, Jeffrey FM, Storey C, Milde A, Koshy S, Lindner J, Magnuson MA, Malloy CR, Sherry AD. Impaired tricarboxylic acid cycle activity in mouse livers lacking cytosolic phosphoenolpyruvate carboxykinase. J Biol Chem 2004;279:48941–48949
24. Mari A, Stojanovska L, Proietto J, Thorburn AW. A circulatory model for calculating non-steady-state glucose fluxes: validation and comparison with compartmental models. Comput Methods Programs Biomed 2003;71: 269–281
25. Edgerton DS, Cardin S, Pan C, Neal D, Farmer B, Converse M, Cherrington AD. Effects of insulin deficiency or excess on hepatic gluconeogenic flux during glycogenolytic inhibition in the conscious dog. Diabetes 2002;51: 3151–3162
26. Moore MC, Satake S, Lautz M, Soleimanpour SA, Neal DW, Smith M, Cherrington AD. Nonesterified fatty acids and hepatic glucose metabolism in the conscious dog. Diabetes 2004;53:32–40
27. Satake S, Moore MC, Igawa K, Converse M, Farmer B, Neal DW, Cherrington AD. Direct and indirect effects of insulin on glucose uptake and storage by the liver. Diabetes 2002;51:1663–1671
28. Goldstein RE, Rossetti L, Palmer BA, Liu R, Massillon D, Scott M, Neal D, Williams P, Peeler B, Cherrington AD. Effects of fasting and glucocorticoids on hepatic gluconeogenesis assessed using two independent methods in vivo. Am J Physiol Endocrinol Metab 2002;283:E946–E957
29. Erion DM, Yonemitsu S, Nie Y, Nagai Y, Gillum MP, Hsiao JJ, Iwasaki T, Stark R, Weismann D, Yu XX, Murray SF, Bhanot S, Monia BP, Horvath TL, Gao Q, Samuel VT, Shulman GI. SirT1 knockdown in liver decreases basal hepatic glucose production and increases hepatic insulin responsiveness in diabetic rats. Proc Natl Acad Sci U S A 2009;106:11288–11293
30. Buettner C, Camacho RC. Hypothalamic control of hepatic glucose production and its potential role in insulin resistance. Endocrinol Metab Clin North Am 2008;37:825–840
31. Pilkis SJ, el-Maghrabi MR, Claus TH. Hormonal regulation of hepatic gluconeogenesis and glycolysis. Annu Rev Biochem 1988;57:755–783
32. Girard J. Metabolic adaptations to change of nutrition at birth. Biol Neonate 1990;58(Suppl. 1):3–15
33. Sindelar DK, Chu CA, Rohlie M, Neal DW, Swift LL, Cherrington AD. The role of fatty acids in mediating the effects of peripheral insulin on hepatic glucose production in the conscious dog. Diabetes 1997;46:187–196
34. Sindelar DK, Balcom JH, Chu CA, Neal DW, Cherrington AD. A comparison of the effects of selective increases in peripheral or portal insulin on hepatic glucose production in the conscious dog. Diabetes 1996;45:1594–1604
35. Barrett EJ, Bevilacqua S, DeFronzo RA, Ferrannini E. Glycogen turnover during refeeding in the postabsorptive dog: implications for the estimation of glycogen formation using tracer methods. Metabolism 1994;43:285–292
36. Jin ES, Uyeda K, Kawaguchi T, Burgess SC, Malloy CR, Sherry AD. Increased hepatic fructose 2,6-bisphosphate after an oral glucose load does not affect gluconeogenesis. J Biol Chem 2003;278:28427–28433
37. Newgard CB, Moore SV, Foster DW, McGarry JD. Efficient hepatic glycogen synthesis in refeeding rats requires continued carbon flow through the gluconeogenic pathway. J Biol Chem 1984;259:6958–6963
38. Sugden MC, Watts DI, Palmer TN, Myles DD. Direction of carbon flux in starvation and after refeeding: in vitro and in vivo effects of 3-mercaptopicolinate. Biochem Int 1983;7:329–337
39. Taylor R, Magnusson I, Rothman DL, Cline GW, Caumo A, Cobelli C, Shulman GI. Direct assessment of liver glycogen storage by 13C nuclear magnetic resonance spectroscopy and regulation of glucose homeostasis after a mixed meal in normal subjects. J Clin Invest 1996;97:126–132
40. Choi IY, Wu C, Okar DA, Lange AJ, Gruetter R. Elucidation of the role of fructose 2,6-bisphosphate in the regulation of glucose fluxes in mice using in vivo (13)C NMR measurements of hepatic carbohydrate metabolism. Eur J Biochem 2002;269:4418–4426
41. Halimi S, Assimacopoulos-Jeannet F, Terrettaz J, Jeanrenaud B. Differential effect of steady-state hyperinsulinaemia and hyperglycaemia on hepatic glycogenolysis and glycolysis in rats. Diabetologia 1987;30:268–272
42. Terrettaz J, Assimacopoulos-Jeannet F, Jeanrenaud B. Inhibition of hepatic glucose production by insulin in vivo in rats: contribution of glycolysis. Am J Physiol 1986;250:E346–E351
43. Le Lay J, Tuteja G, White P, Dhir R, Ahima R, Kaestner KH. CRTC2 (TORC2) contributes to the transcriptional response to fasting in the liver but is not required for the maintenance of glucose homeostasis. Cell Metab 2009;10:55–62
44. Hendrick GK, Frizzell RT, Williams PE, Cherrington AD. Effect of hyperglucagonemia on hepatic glycogenolysis and gluconeogenesis after a prolonged fast. Am J Physiol 1990;258:E841–E849
45. Rothman DL, Magnusson I, Katz LD, Shulman RG, Shulman GI. Quantitation of hepatic glycogenolysis and gluconeogenesis in fasting humans with 13C NMR. Science 1991;254:573–576
46. Blackshear PJ, Holloway PA, Aberti KG. The effects of inhibition of gluconeogenesis on ketogenesis in starved and diabetic rats. Biochem J 1975;148:353–362
47. DiTullio NW, Berkoff CE, Blank B, Kostos V, Stack EJ, Saunders HL. 3-mercaptopicolinic acid, an inhibitor of gluconeogenesis. Biochem J 1974;138:387–394
48. Ferre P, Pegorier JP, Girard J. The effects of inhibition of gluconeogenesis in suckling newborn rats. Biochem J 1977;162:209–212
49. Burgess SC, He T, Yan Z, Lindner J, Sherry AD, Malloy CR, Browning JD, Magnuson MA. Cytosolic phosphoenolpyruvate carboxykinase does not solely control the rate of hepatic gluconeogenesis in the intact mouse liver. Cell Metab 2007;5:313–320
50. Defronzo RA. Banting Lecture: From the triumvirate to the ominous octet: a new paradigm for the treatment of type 2 diabetes mellitus. Diabetes 2009;58:773–795
51. Korsheninnikova E, Voshol PJ, Baan B, van der Zon GC, Havekes LM, Romijn JA, Maassen JA, Ouwens DM. Dynamics of insulin signalling in liver during hyperinsulinemic euglycaemic clamp conditions in vivo and the effects of high-fat feeding in male mice. Arch Physiol Biochem 2007;113:173–185
52. Ropelle ER, Pauli JR, Cintra DE, Frederico MJ, de Pinho RA, Velloso LA, De Souza CT. Acute exercise modulates the Foxo1/PGC-1alpha pathway in the liver of diet-induced obesity rats. J Physiol 2009;587:2069–2076
53. Samuel VT, Beddow SA, Iwasaki T, Zhang XM, Chu X, Still CD, Gerhard GS, Shulman GI. Fasting hyperglycemia is not associated with increased expression of PEPCK or G6Pc in patients with type 2 diabetes. Proc Natl Acad Sci U S A 2009;106:12121–12126